

File Unit

AD-A217 168

ELECTROCHEMICAL PHASE DIAGRAMS  
FOR AQUEOUS REDOX SYSTEMS

JOHN C. ANGUS  
MICHAEL J. ZAPPIA  
REBECCA C. YUNG

DECEMBER 22, 1989

U.S. ARMY RESEARCH OFFICE  
GRANT: DAAL03-86-K-0062

CASE WESTERN RESERVE UNIVERSITY  
CLEVELAND, OH 44106

APPROVED FOR PUBLIC RELEASE,  
DISTRIBUTION UNLIMITED

OTIC  
JAN 23 1990

90 01 22 187

UNCLASSIFIED

SECURITY CLASSIFICATION OF THIS PAGE (When Data Entered)

REPORT DOCUMENTATION PAGE		READ INSTRUCTIONS BEFORE COMPLETING FORM
1. REPORT NUMBER <i>ARO 23359.1-MS</i>	2. GOVT ACCESSION NO. N/A	3. RECIPIENT'S CATALOG NUMBER N/A
4. TITLE (and Subtitle) ELECTROCHEMICAL PHASE DIAGRAMS FOR AQUEOUS REDOX SYSTEMS		5. TYPE OF REPORT & PERIOD COVERED Final 8/1/86 to 7/31/89
		6. PERFORMING ORG. REPORT NUMBER
7. AUTHOR(s) John C. Angus Michael J. Zappia Rebecca C. Yung		8. CONTRACT OR GRANT NUMBER(s) DAAL03-86-K-0062
9. PERFORMING ORGANIZATION NAME AND ADDRESS Case Western Reserve University Cleveland, OH 44106		10. PROGRAM ELEMENT, PROJECT, TASK AREA & WORK UNIT NUMBERS
11. CONTROLLING OFFICE NAME AND ADDRESS U. S. Army Research Office Post Office Box 12211 Research Triangle Park, NC 27709		12. REPORT DATE December 22, 1989
		13. NUMBER OF PAGES 27
14. MONITORING AGENCY NAME & ADDRESS (if different from Controlling Office)		15. SECURITY CLASS. (of this report) Unclassified
		15a. DECLASSIFICATION/DOWNGRADING SCHEDULE
16. DISTRIBUTION STATEMENT (of this Report)  Approved for public release; distribution unlimited.		
17. DISTRIBUTION STATEMENT (of the abstract entered in Block 20, if different from Report)  NA		
18. SUPPLEMENTARY NOTES  The view, opinions, and/or findings contained in this report are those of the author(s) and should not be construed as an official Department of the Army position, policy, or decision, unless so designated by other documentation.		
19. KEY WORDS (Continue on reverse side if necessary and identify by block number) Electron Number Diagrams Potential-pH Diagrams Corrosion Aqueous Redox Systems		
20. ABSTRACT (Continue on reverse side if necessary and identify by block number)  A completely new phase diagram, the electron number diagram, has been developed for aqueous redox systems. The electron number diagram is a transformed potential-pH diagram in which potential is replaced by its thermodynamic conjugate, the number of electrons. The relationship between electron number diagrams and potential-pH diagrams, which provide complementary information, is explained in thermodynamic and geometric terms.  Electron number diagrams show many similarities to metallurgical T-x		

diagrams. Because electron number is a conserved quantity, material balances can be performed on electron number diagrams, and process trajectories can be followed. The mass and electron balance equations are derived, and electron number diagrams are used to illustrate a variety of process trajectories. The diagrams are of particular value in describing the complex phase chemistry involved in aqueous corrosion, hydrometallurgical ore processing, nuclear waste disposal, geochemical processes and some fuel sulfur removal processes.

Experimental electron number diagrams for the aqueous sulfur system were determined. The measured and computed diagrams are in good agreement. Comparison of the measured and computed diagrams permit conclusions to be drawn about chemical processes taking place in the system.

A detailed thermodynamic analysis of complex aqueous redox systems was the basis for algorithms for construction of generalized chemical potential diagrams, potential-pH diagrams and electron number diagrams. Extremely efficient computer programs based on the algorithms were used to construct diagrams for a variety of systems, including the following which include two active redox elements: the aqueous U-C, Cd-Te and Ga-As systems. Extension of these algorithms to systems of arbitrary complexity is also discussed. (1.0) ✓

## TABLE OF CONTENTS

1.0	STATEMENT OF PROBLEM STUDIED	1
2.0	SUMMARY OF MOST IMPORTANT RESULTS	1
	2.1 Conclusions	
	2.2 Recommendations	
3.0	LIST OF PUBLICATIONS AND TECHNICAL PRESENTATIONS	3
	3.1 Papers Published in Refereed Journals	
	3.2 Papers Published in Conference Proceedings	
	3.3 Computer Programs to be Published	
	3.4 Completed Theses	
4.0	PARTICIPATING SCIENTIFIC PERSONNEL	4
5.0	COMPUTED ELECTROCHEMICAL PHASE DIAGRAMS	4
	5.1 Electron Number Diagrams	
	5.2 Potential-pH Diagrams	
	5.3 Chemical Potential Diagrams	
6.0	MEASURED ELECTRON NUMBER DIAGRAM FOR THE AQUEOUS SULFUR SYSTEM	5
7.0	REFERENCES	6
8.0	FIGURES	7



Preparation For	
<input checked="" type="checkbox"/> DTIC <input type="checkbox"/> Other	<input checked="" type="checkbox"/> <input type="checkbox"/>
Ex. _____ Library Number/	
Availability Codes	
Main and/or	
Dist	Special
A-1	

## 1.0 STATEMENT OF PROBLEM STUDIED

A phase diagram is a useful means of summarizing a large amount of thermodynamic information in a convenient, compact form. This thermodynamic information can be used to understand the behavior of complex systems, to plan experiments and to interpret experimental data. Although kinetic information is necessary to determine the rates at which chemical reactions occur in a system, a thermodynamic analysis can provide insight into the energetically allowed possibilities.

Various types of phase diagrams have been developed for electrochemical systems. Potential-pH diagrams, which display the stability of chemical species on a field of potential vs. pH, have been applied to corrosion studies, hydrometallurgy, geologic studies and electrodeposition. In these and other applications, potential-pH diagrams have been successfully used in the prediction of behavior, the determination of conditions for experimental studies and the interpretation of experimental results.

Several factors have limited the usefulness of potential-pH diagrams. Inconsistencies in the methods used to compute and present potential-pH diagrams have caused great confusion in their interpretation. Furthermore, the link between the phase behavior of electrochemical systems and these diagrams has not always been clear. Additionally, potential-pH diagrams are inconvenient or inappropriate in some applications because potential is not a conserved quantity. Improvements in these areas would increase the utility of electrochemical phase diagrams as tools for the study of aqueous redox systems.

The purpose of this work is to improve the understanding of electrochemical phase diagrams for aqueous redox systems by developing: (1) a thermodynamic framework for the study of aqueous redox systems; (2) new electrochemical phase diagrams; and (3) efficient methods of computing electrochemical phase diagrams.

## 2.0 SUMMARY OF MOST IMPORTANT RESULTS

### 2.1 Conclusions

The conclusions drawn from this study may be summarized as follows:

1. An entirely new type of electrochemical phase diagram, the electron number diagram, has been discovered. The theoretical foundation for electron number diagrams and their relationship to conventional potential-pH diagrams have been developed. The areas in which electron number diagrams provide information complementary to and in addition to that from conventional potential-pH diagrams have been identified.

2. An experimental verification of the electron number diagram for one redox system, the aqueous sulfur system, has been accomplished. Two-dimensional sections of the three-dimensional electron number diagram at both constant pH and constant electron number were determined and compared with the sections computed from theory. Good agreement between the computed and measured diagrams was found.

3. A rigorous thermodynamic theory for complex aqueous redox systems was developed and used for interpretation of the various types of electrochemical phase diagrams. The dimensionality of potential-pH and electron number diagrams was related to the Gibbs phase rule analysis of aqueous redox systems. The theoretical analysis permits a classification of potential-pH diagrams into two basic types: 1) Pourbaix diagrams, in which

the stability field of solid phases and contours of constant activity of the redox element are displayed and 2) predominance diagrams, in which the regions of dominance of dissolved species are shown. Electron number diagrams are obtained by a thermodynamic transformation of the potential to its thermodynamic conjugate variable, the electron number.

4. An efficient computational method, based on the theoretical analysis of complex aqueous redox systems, was developed. The equations describing the equilibrium composition were obtained from a minimum set of formation reactions. The formation reactions used a set of reactants (components) whose chemical potentials are chosen to be the independent variables in the computation. This procedure permits the sequential, rather than simultaneous, solution of the equation set in the case of ideal solutions. Efficient stability criteria, obtained from theory, were used to determine the stability of solid phases. The algorithm was implemented on IBM PCs and compatible computers.

5. Electron number, potential-pH and chemical potential diagrams were computed for a variety of complex aqueous systems, including the following systems containing two active redox elements: the aqueous Cd-Te system; the aqueous Ga-As system; and the aqueous U-C system.

## 2.2 Recommendations

Further development of the work described in this report is recommended. The following specific items are particularly important.

1. Develop methods for computation and display of electron number diagrams for solid-aqueous redox systems containing three or more active redox elements. These will be necessary for many corrosion, geological and mineral processing applications.

2. Develop algorithms for computation and display of generalized chemical potential/temperature/pressure diagrams. These "intensive property" diagrams will contain conventional Pourbaix and Ellingham diagrams as subsets.

3. Improve the data-base supporting the computations by providing an interface to the most recent compilations of thermodynamic data, e.g., that of the National Institute for Standards and Technology (Wagman et al., 1982; Wang and Neumann, 1989). The algorithms should also be extended by building in methods for computing activity coefficients and for extrapolating data to elevated temperatures.

4. Additional experimental confirmation of electron number diagrams should be obtained. The aqueous system containing copper and chlorine should exhibit many interesting phase phenomena in a region that is easily accessible experimentally. Work on the aqueous sulfur system should be expanded and should include: 1) development of a more complete data base to support the computed diagrams and 2) more accurate potential measurements.

5. Additional applications for electron number diagrams should be sought and developed. These might be drawn from the following fields: corrosion, nuclear waste containment, wet sulfur removal processes and electroplating of III-V semiconductor compounds.

6. Extension of the concept of electron number diagrams to non-aqueous systems, e.g., molten salts and organic solvents, should be explored.

### 3.0 LIST OF PUBLICATIONS AND TECHNICAL PRESENTATIONS

#### 3.1 Papers Published in Refereed Journals

The following research papers describe work supported under the Department of Army research grant DAAL03-86-K-0062 and the preceding grant DAAG29-84-K-0074.

1. John C. Angus and Charles T. Angus, "Computation of Pourbaix Diagrams Using Virtual Species: Implementation on Personal Computers," J. Electrochem. Soc., 132(5) 1014-19 (1985).
2. John C. Angus, Bei Lu and Michael J. Zappia, "Potential-pH Diagrams for Complex Systems," J. Appl. Electrochem., 17, 1-21 (1987).
3. John C. Angus and Michael J. Zappia, "Electron Number Diagrams: A Transformed Potential-pH Diagram," J. Electrochem. Soc., June, 1987.

#### 3.2 Papers Published in Conference Proceedings

The following research papers describing work done under Department of Army support appeared in published conference proceedings:

4. John C. Angus and Michael J. Zappia, "Electron Number Diagrams: A Transformed Potential-pH Diagram," Proceedings of Pourbaix Symposium, Electrochemical Society Meeting, New Orleans, LA, pp. 59-68, October, 1984.
5. John C. Angus and Charles T. Angus, "Computation of Pourbaix Diagrams Using Virtual Species: Implementation on Personal Computers," Proceedings of Pourbaix Symposium, Electrochemical Society Meeting, New Orleans, LA, pp. 109-24, October, 1984.
6. John C. Angus, Michael J. Zappia and Charles T. Angus, "Electron Number and Potential-pH Diagrams," Proceedings of International Conference on Corrosion Science and Technology, Calcutta, India, p. 11, February 21-23, 1985.
7. John C. Angus, Michael J. Zappia and Bei Lu, "Computed Phase Diagrams for Complex Aqueous/Solid Redox Systems: Applications to Corrosion Processes," invited paper, Tri Services Conference on Corrosion, Orlando, FL, December 5, 1985.
8. John C. Angus and Michael J. Zappia, "Electron Number Diagrams: A New Phase Diagram for Complex Aqueous Redox Systems," AIChE 1986 Annual Meeting, Miami, FL, November 3, 1986.
9. Michael J. Zappia, John C. Angus and Rebecca Yung, "The Electron Number Diagram: A New Tool for the Analysis of Aqueous Redox Systems," 1989 Tri-Service Corrosion Conference, October 17-19, 1989.

#### 3.3 Computer Programs to be Published

The computer programs together with a detailed description of the underlying thermodynamic theory will be published by John Wiley & Sons Ltd., London, UK during 1990. The publication will include program disks, manual and theoretical discussion:

10. John C. Angus, Michael J. Zappia and Bei Lu, "Electrochemical Phase Diagrams, John Wiley & Sons Ltd., London, UK, to be published 1990.

### 3.4 Completed Theses

The following theses have been completed under the Department of Army support. These theses, especially the Ph.D. thesis of Dr. Michael J. Zappia, are the major repository of the work done under this project.

Bei Lu, M.S. Thesis, "Computer Computation of Pourbaix Diagrams, Predominance Diagrams and Electron Number Diagrams for Complex Systems," November, 1985.

Rebecca C. Yung, M.S. Thesis, "The Experimental Determination of Electron Number Diagrams for the Aqueous-Sulfur System," November, 1989 (degree dated January, 1990).

Michael J. Zappia, Ph.D. Thesis, "Electrochemical Phase Diagrams for Aqueous Redox Systems" December, 1989. (degree dated May, 1990).

### 4.0 PARTICIPATING SCIENTIFIC PERSONNEL

The following scientific personnel participated in the project:

Professor John C. Angus, Principal Investigator

Dr. Michael J. Zappia  
Earned Ph.D. Degree under project

Mr. Bei Lu  
Earned M.S. Degree under project

Ms. Rebecca C. Yung  
Earned M.S. Degree under project

Ms. Vicky Garcia  
Earned M.S. Degree under project

Mr. Terry L. Stover

### 5.0 COMPUTED ELECTROCHEMICAL PHASE DIAGRAMS

#### 5.1 Electron Number Diagrams

A selection of electron number diagrams for the aqueous copper, sulfur, uranium and chromium systems is given in Section 7.0. Captions on the figures indicate various process trajectories. A more detailed discussion of the diagrams may be found in reference 3 cited in section 3.1 and in the Ph.D. thesis of Dr. M.J. Zappia cited in section 3.4.

When interpreting the electron number diagrams, note that the electron number,  $\bar{z}$ , is numerically equal to the number average electrochemical valence,  $z_1$

$$\bar{z}_j = \frac{\sum N_i \alpha_{ij} z_i}{\sum N_i \alpha_i}$$

where  $N_i$  is the number of moles of species  $i$ ,  $\alpha_{ij}$  the number of atoms of element  $j$  in one molecule of species  $i$  and  $z_i$  the electrochemical valence of element  $j$  in species  $i$ .

For example an equimolar mixture of  $\text{Cu}_2\text{O}$  and  $\text{CuO}$  would have the following electron number for copper:

$$z_{\text{Cu}} = \frac{(1)(2)(1) + (1)(1)(2)}{(1)(2) + (1)(1)} = \frac{4}{3}$$

An equimolar mixture of  $\text{Cu}^+$  and  $\text{Cu}^{++}$  ions would have an electron number for copper of

$$z_{\text{Cu}} = \frac{(1)(1)(1) + (1)(1)(2)}{(1)(1) + (1)(1)} = 1.5$$

## 5.2 Potential-pH Diagrams

A selection of potential -pH diagrams for complex mixtures is also shown in section 7.0. These were all constructed using the methods developed under the grant. Further description of these diagrams can be found in references 1 and 2 cited in section 3.1 and in the Ph.D. thesis of Dr. M.J. Zappia cited in section 3.4.

## 5.3 Chemical Potential Diagrams

A selection of several generalized chemical potential diagrams is also given in Section 7.0. These diagrams are described more fully in the Ph.D. thesis of Dr. M.J. Zappia cited in section 3.4.

# 6.0 **MEASURED ELECTRON NUMBER DIAGRAM FOR THE AQUEOUS SULFUR SYSTEM**

## 6.1 General Discussion of Method

Two types of experiments have been used to construct experimental electron number diagrams for the aqueous sulfur system. In both types of experiments, the boundary between the single phase aqueous region and the two phase region where solid sulfur exists in equilibrium with dissolved sulfur was determined. In an *indirect* determination experiment, acidification of the starting solution caused the precipitation of solid sulfur. The distribution of sulfur between the solid and aqueous phases was then used together with mass and electron balances to determine a point on the phase boundary. The second type of experiment involved a *direct* visual determination of whether or not solid sulfur had formed. By determining points inside and outside the two phase region, the position of the phase boundary could be inferred.

## 6.2 Equipment and Procedure

The same experimental apparatus was used for both types of experiments. It consisted of a 250 ml glass jar with a Teflon-lined phenolic screw cap. Electrodes, burets and pipets were inserted through holes in the cap; O-rings on these inserts were clamped against the

top of the cap to limit gas flow between the jar and the outside environment. The unused holes were tightly stoppered during the experimental runs. The apparatus is shown schematically in Figure 6-1.

Potential and pH measurements were made using an Orion EA940 IonAnalyzer. This meter was connected via a serial port to a microcomputer, allowing automated collection and storage of data. The combination pH electrodes used were Orion model 91-06 and Fisher AccupHast model 13-620-281. An Orion Platinum Redox Electrode (model 96-78) was also used in most of the indirect experiments.

To aid in the detection of small quantities of solid in dilute solutions, a 5-mW helium-neon laser (Uniphase Model 1105P,  $\lambda = 633\text{nm}$ ) was used. The beam was directed through the experimental solution in a darkened room and observed at a  $90^\circ$  angle to the direction of the incident beam. Colloidal sulfur particles caused scattering that was visible as a line through the solution. The experimental solutions were compared to "background" solutions which contained comparable concentrations of sulfur species and NaCl, but which were kept at high pH where solid sulfur did not form.

### 6.3 Measured Diagrams

Two examples of measured electron number diagrams for the sulfur system are shown in Figures 6-1 and 6-2. They are two dimensional intersections of the full three dimensional diagram (Figure 5.2) with planes of constant  $\text{pH} = 4.7 \pm 0.5$  and  $\bar{z} = -1.85$  respectively. A discussion of sources of error and other experimental details is given in the M.S. thesis of Bei Lu and the Ph.D. thesis of M.J. Zappia cited in section 3.4 of this report.

## 7.0 REFERENCES

Wagman, D.D., Evans, W.H., Parker, V.P. Schumm, R.H., Halow, I., Bailey, S.M., Churney, K.L., Nuttal, R.L., J. Phys. Chem. Ref. Data, Vol. II, Supp. No. 2, 1982.

Wang, P., Neumann, D.B., J. Chem. Inf. Comput. Sci. 1989, 29, 31.

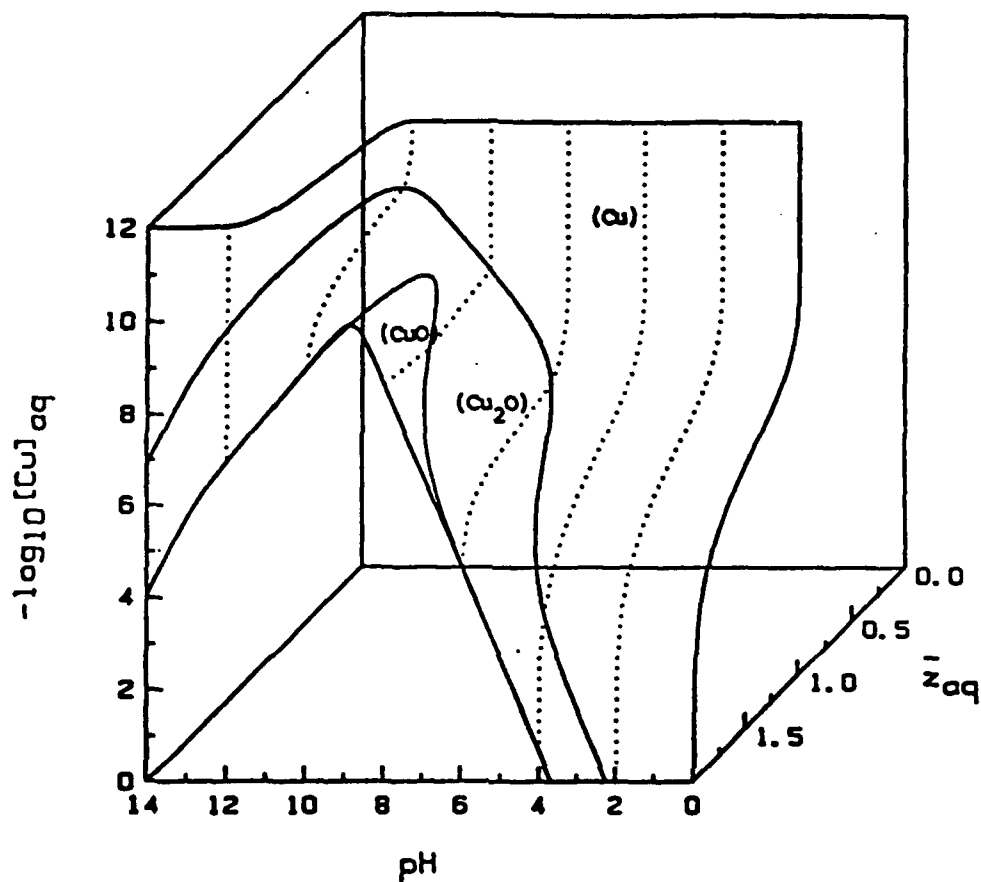
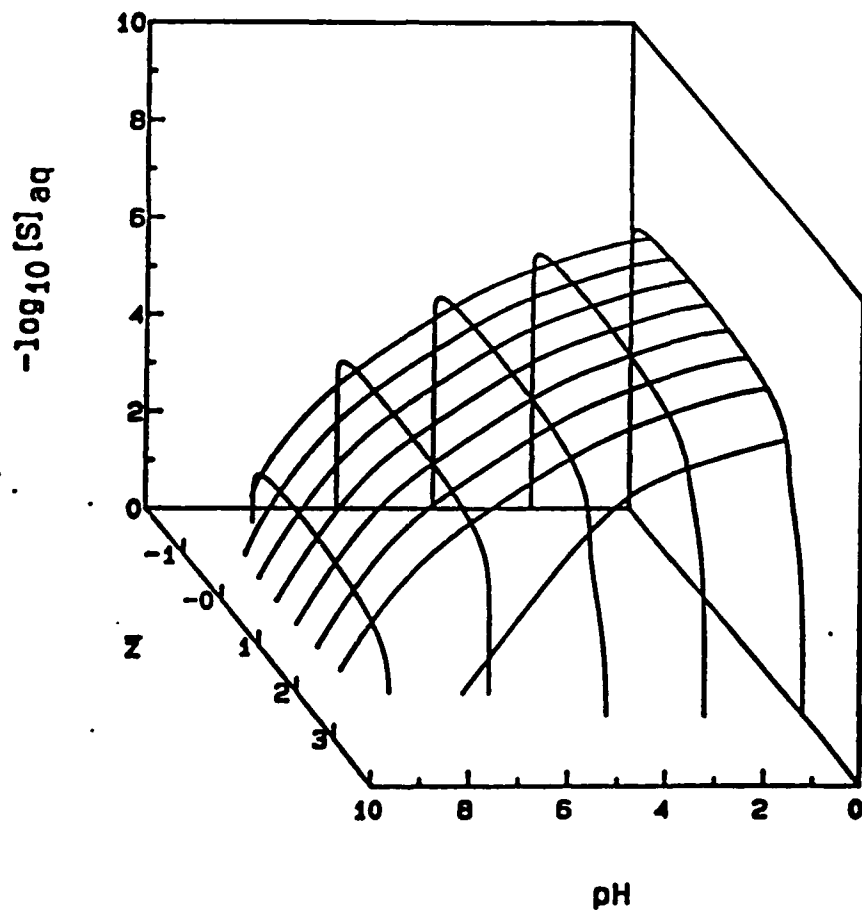


Figure 5-1 Three dimensional electron number diagram for the aqueous copper system. The surface shows the electron number of the aqueous phase in equilibrium with stable copper-containing solids. The solids in parentheses are in equilibrium with the designated sections of the aqueous surface.



**Figure 5-2** Three dimensional electron number diagram for the aqueous sulfur system. The surface shows the electron number of the aqueous phase in equilibrium with solid S ( $z = 0$ ).

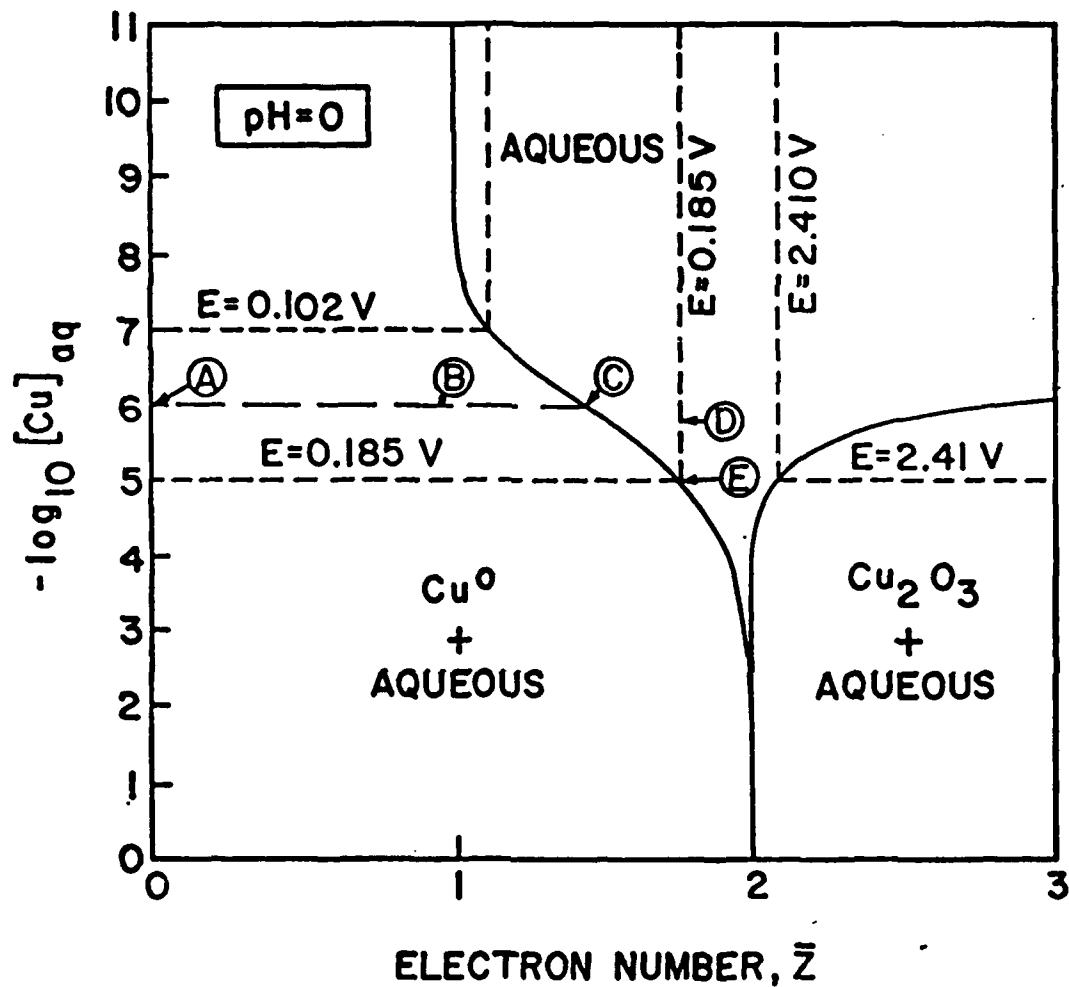


Figure 5-3 Electron number diagram for the copper system. Intersection of the three dimensional figure with the  $\text{pH} = 0$  plane. Equilibrium line of a solution with  $[\text{Cu}]_{\text{aq}} = 10^{-6}$  molal with solid Cu is shown along line  $\overline{ABC}$ . Evaporation trajectory at constant  $\bar{z} = 1.75$  is shown along the line  $\overline{DE}$ .

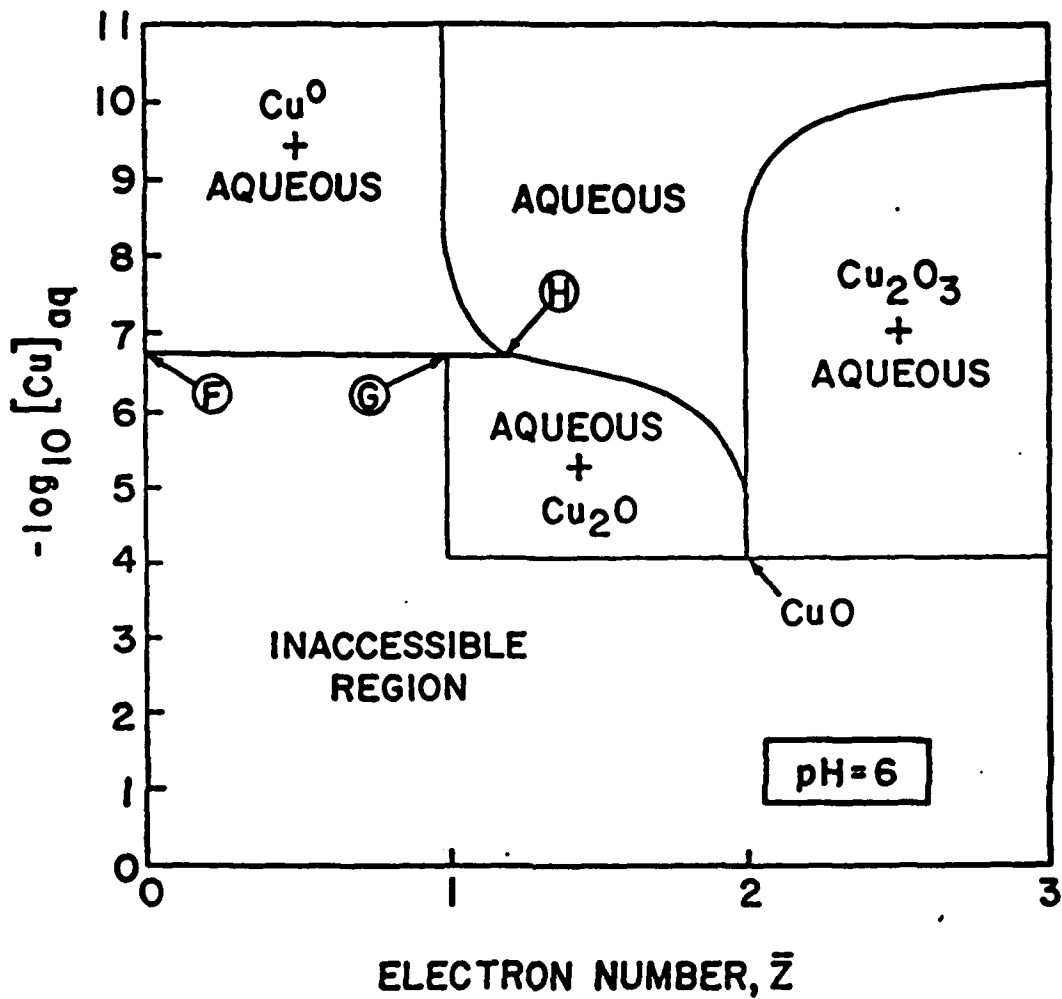


Figure 5-4 Electron number diagram for the copper system. Intersection of the three dimensional figure with the  $\text{pH} = 6$  plane. Note the peritectic reaction between  $\text{Cu}$ ,  $\text{Cu}_2\text{O}$  and the aqueous phase along the line  $\overline{\text{FGH}}$ .

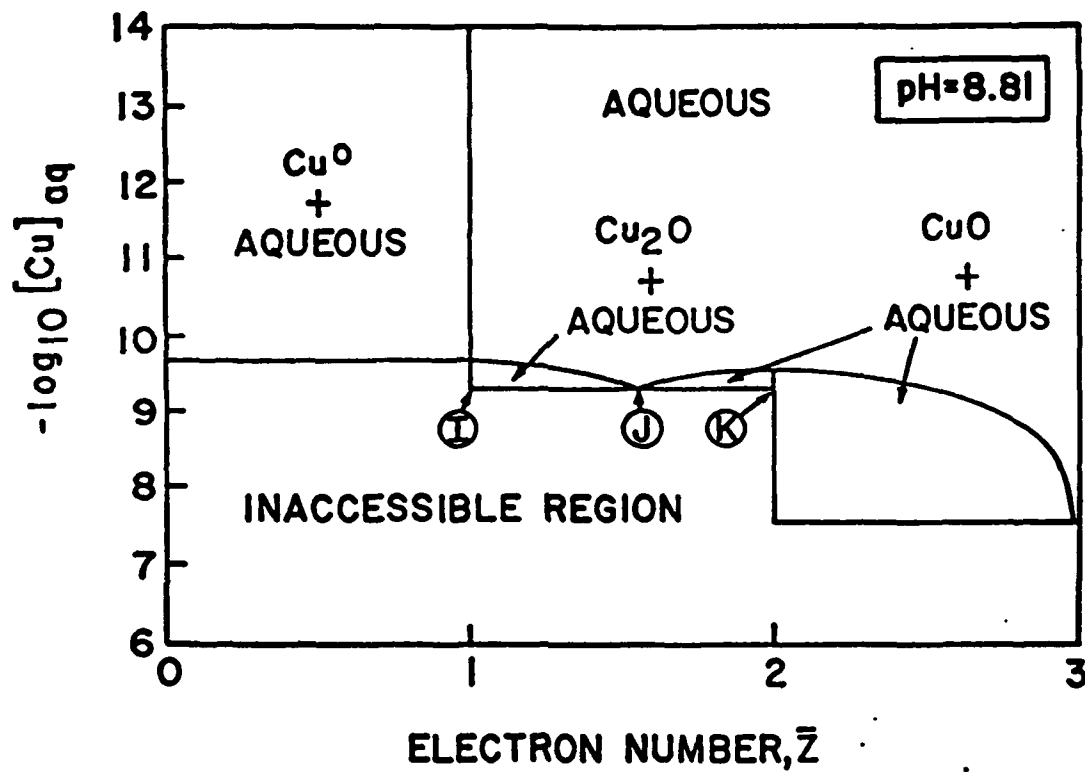


Figure 5-5 Electron number diagram for the copper system. Intersection of the three dimensional figure with the  $\text{pH} = 8.81$  plane. Note the eutectic reaction between  $\text{Cu}_2\text{O}$ , the aqueous phase and  $\text{CuO}$  along the line IJK.

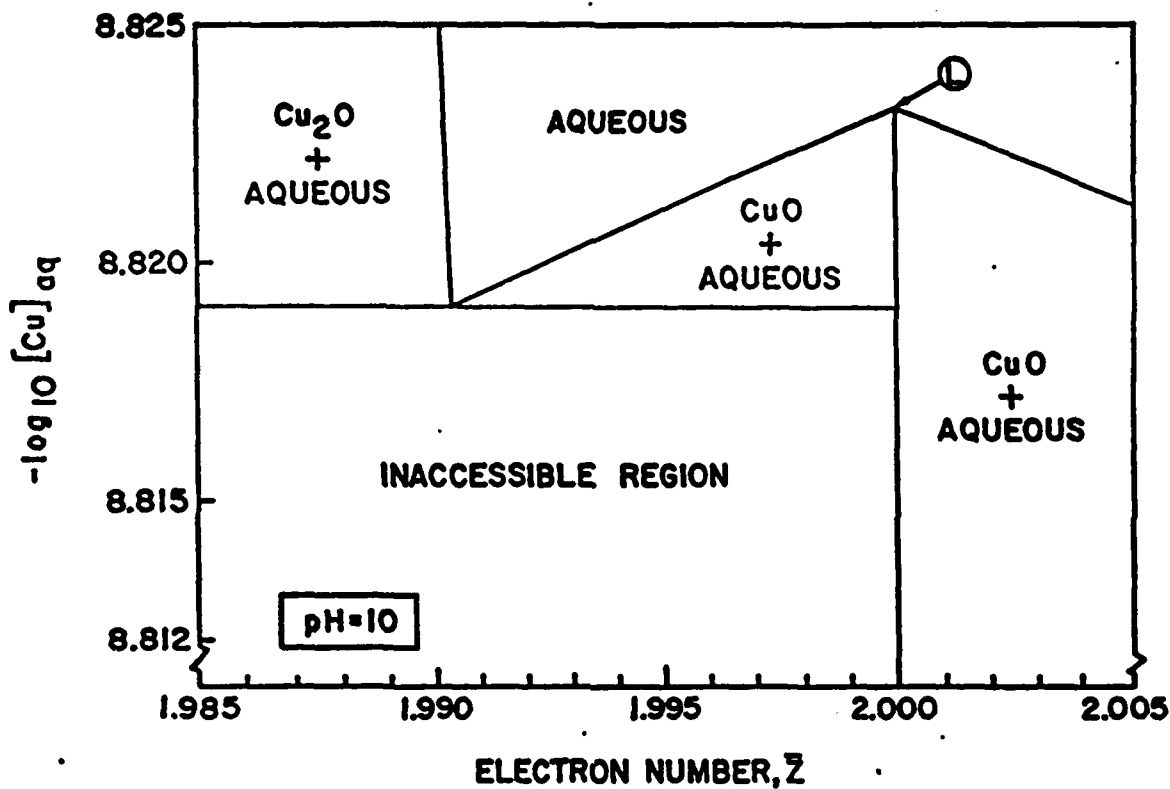


Figure 5-6 Electron number diagram for the copper system. Intersection of the three dimensional figure with the  $\text{pH} = 10$  plane. Detail of electron number diagram near  $\bar{z} = 2$ . Note the congruent type dissolution of  $\text{CuO}$  at point L and the eutectic type reaction between  $\text{Cu}_2\text{O}$ , the aqueous phase and  $\text{CuO}$ .

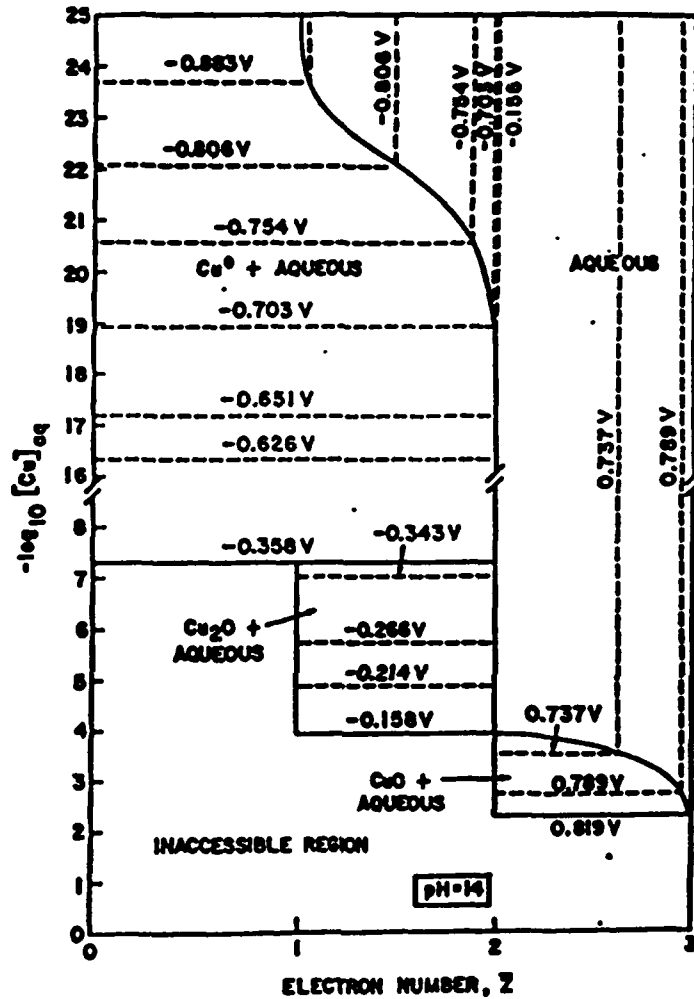


Figure 5-7 Electron number diagram for the copper system. Intersection of the three dimensional figure with the  $pH = 14$  plane. Constant potential lines are shown.

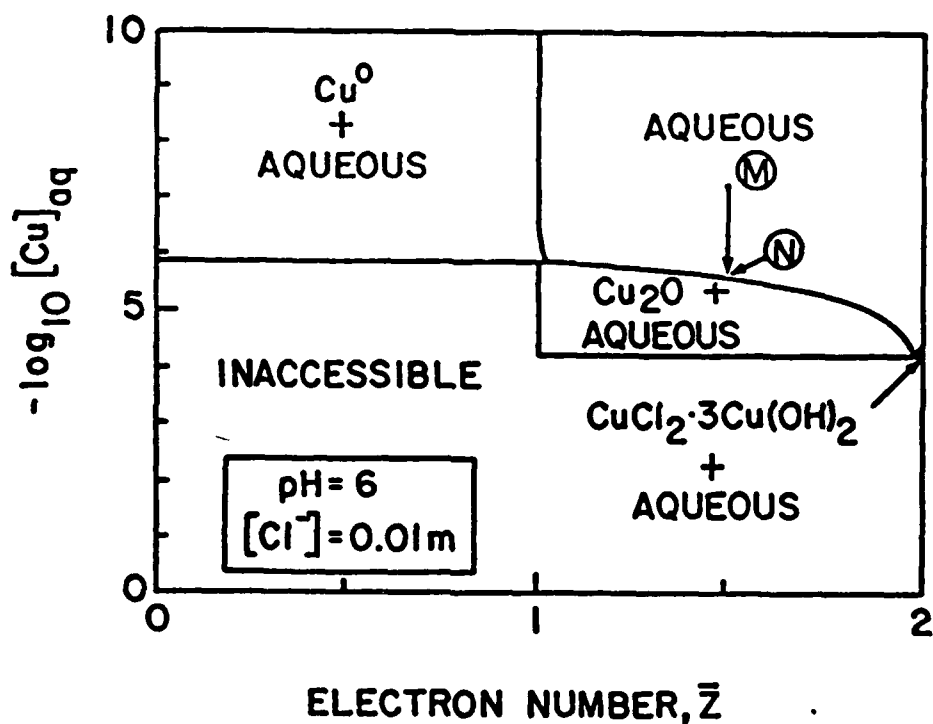


Figure 5-8 Electron number diagram for the copper system. Intersection of the three dimensional figure with the  $\text{pH} = 6$  plane. The chloride ion concentration is 0.01 molal. Evaporation of a solution with  $\bar{z} = 1.5$  at constant  $\text{pH}$  and  $\bar{z}$  follows the line  $\overline{MN}$ . Solid  $\text{Cu}_2\text{O}$  precipitates out at point N.

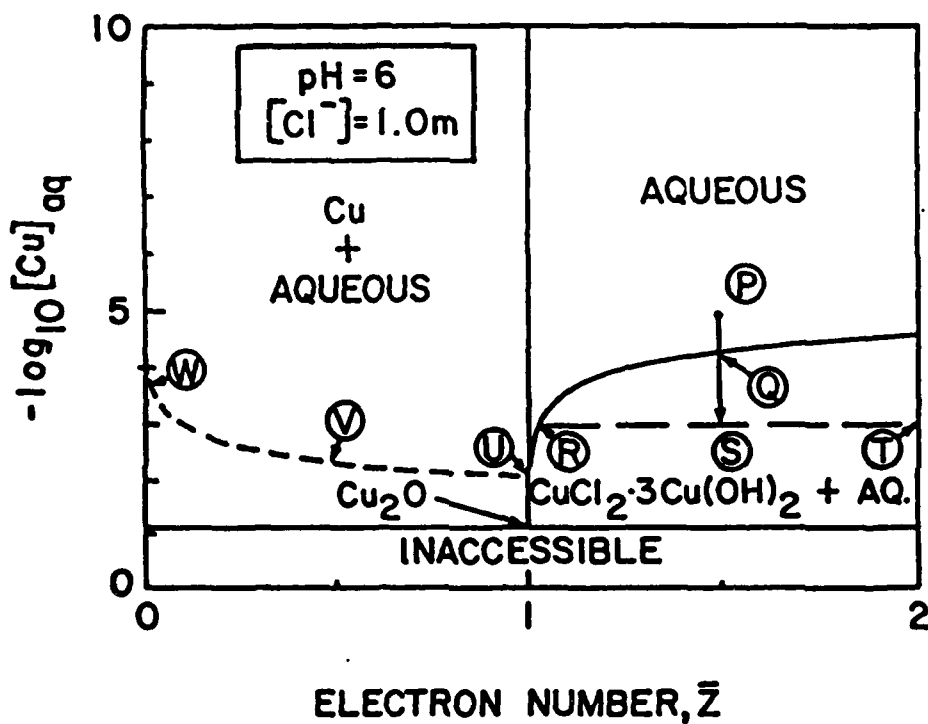


Figure 5-9 Electron number diagram for the copper system. Intersection of the three dimensional figure with the  $\text{pH} = 6$  plane. The chloride ion concentration is 1.0 molal. The evaporation trajectory along a path of constant  $\bar{z} = 1.5$  is shown along line  $\overline{\text{PQS}}$ . The final equilibrium state is along the line  $\overline{\text{RST}}$ . The trajectory followed during electroplating of a solution with original concentration of 0.01 molal dissolved copper is shown along the line  $\overline{\text{UVW}}$ .

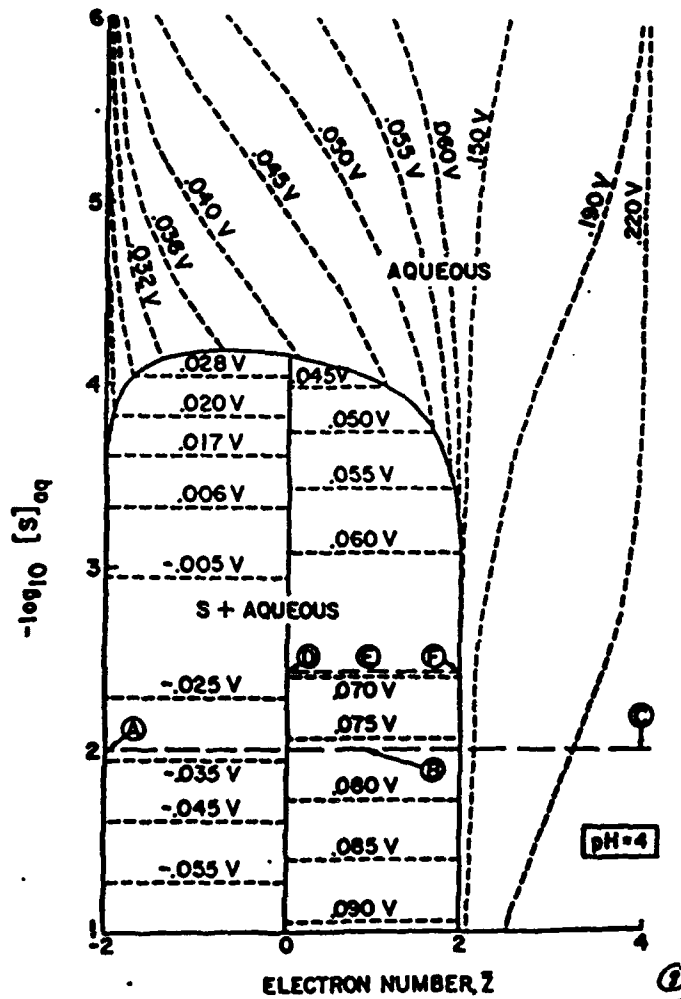


Figure 5-10 Electron number diagram for the sulfur system. Intersection of the three dimensional figure with the  $\text{pH} = 4$  plane. The mixing of equal amounts of 0.01 molal solutions of  $\text{S}^{2-}$  (point A) and  $\text{SO}_3^{2-}$  (point C) to give a mixing point of B is illustrated. Because of precipitation of solid sulfur the final system point moves to E. In the final equilibrium state a two phase system along line  $\overline{DEF}$  exists.

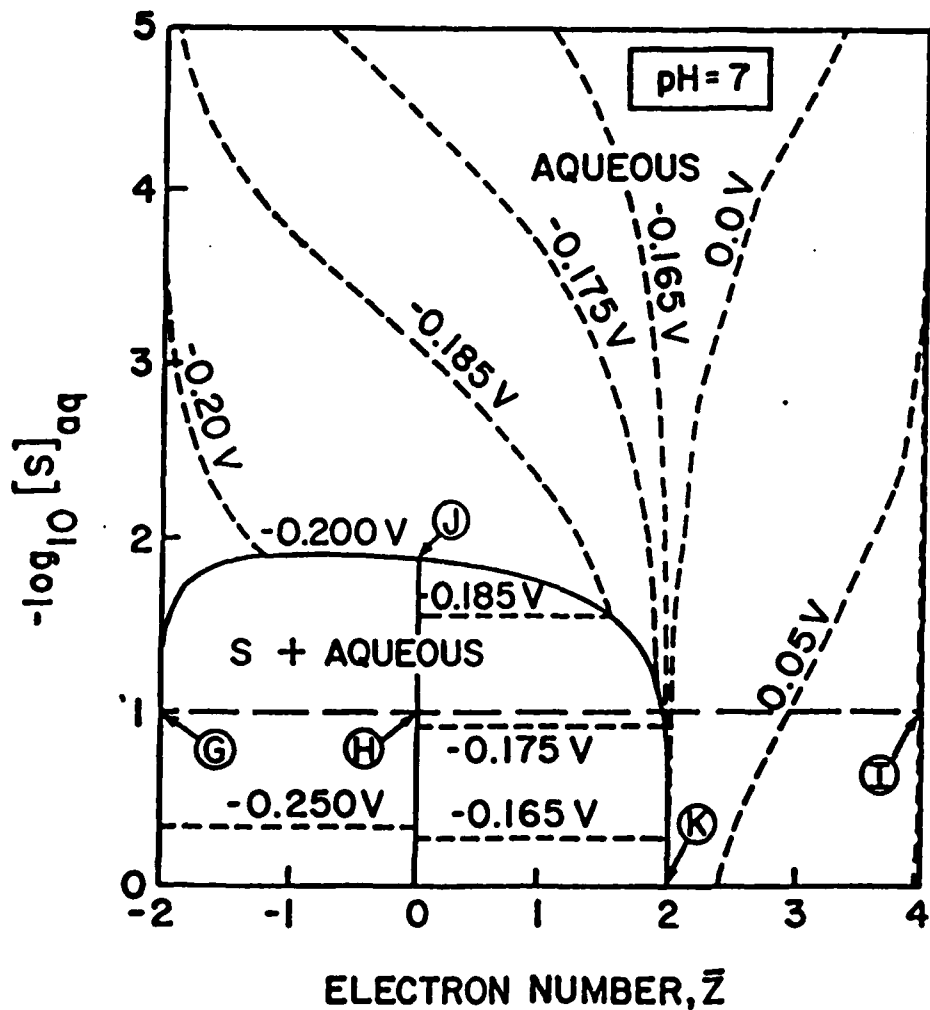


Figure 5-11 Electron number diagram for the sulfur system. Intersection of the three dimensional figure with the  $\text{pH} = 7$  plane. Bisulfate and sulfate ions are not included in the calculation. The mixing of 0.1 molal solutions of  $\text{S}^{2-}$  (point G) and  $\text{SO}_3^{2-}$  (point I) in the ratio of 2/1 to give a mixing point at H with  $\bar{z} = 0$  is shown. Because of the requirement that the solution have  $\bar{z}_{aq} = 0$ , the final state of the solution is at point J.

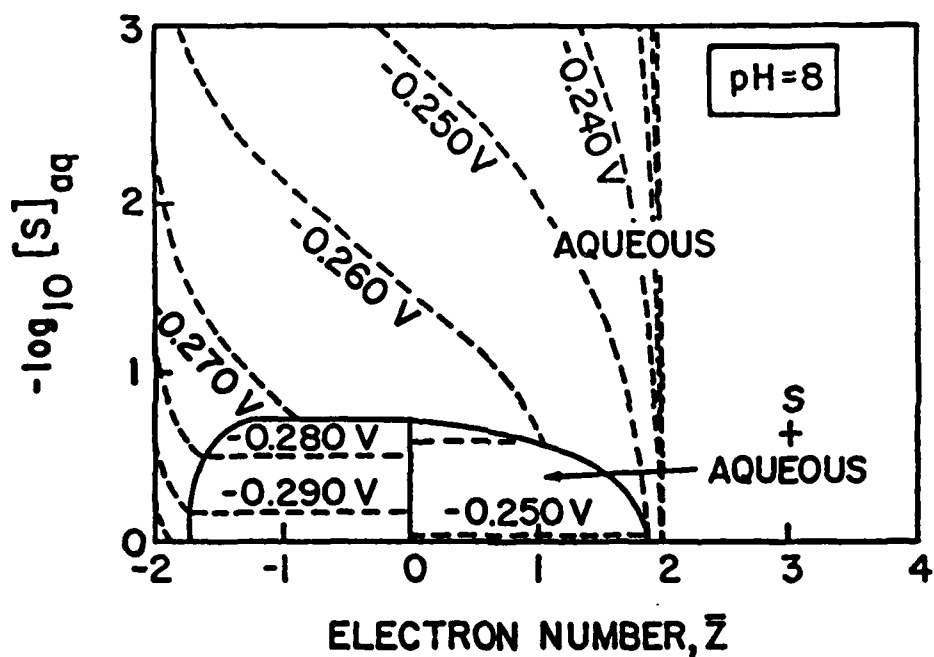


Figure 5-12a Electron number diagram for the sulfur system. Intersection of the three dimensional figure with the pH = 8 plane. Bisulfate and sulfate ions are not included in the calculation.

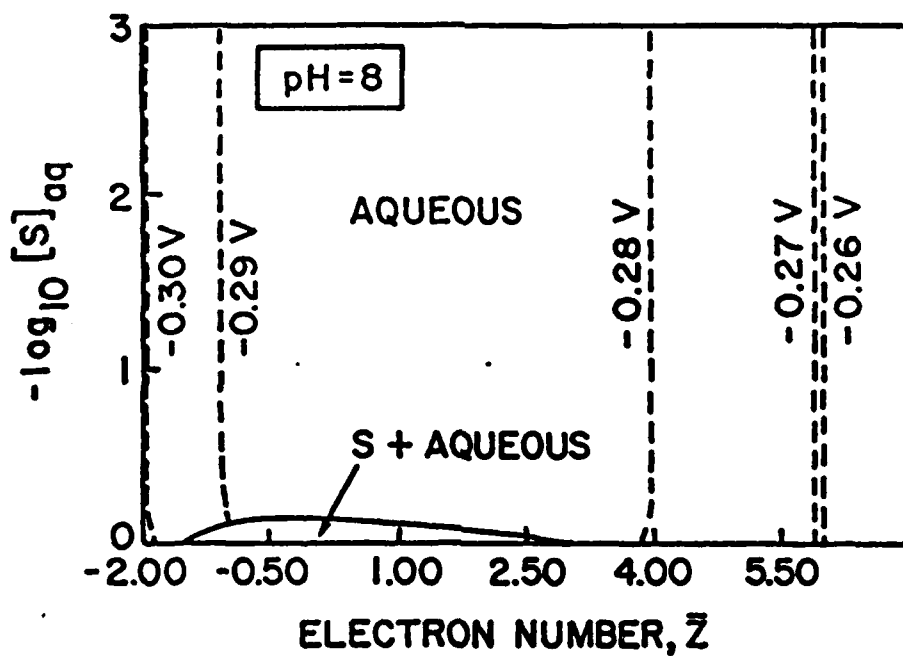


Figure 5-12b Electron number diagram for the sulfur system. Intersection of the three dimensional figure with the  $\text{pH} = 8$  plane. Bisulfate and sulfate ions are included in the calculation. Note the greatly increased solubility of sulfur compared to that shown in Figure 10a.

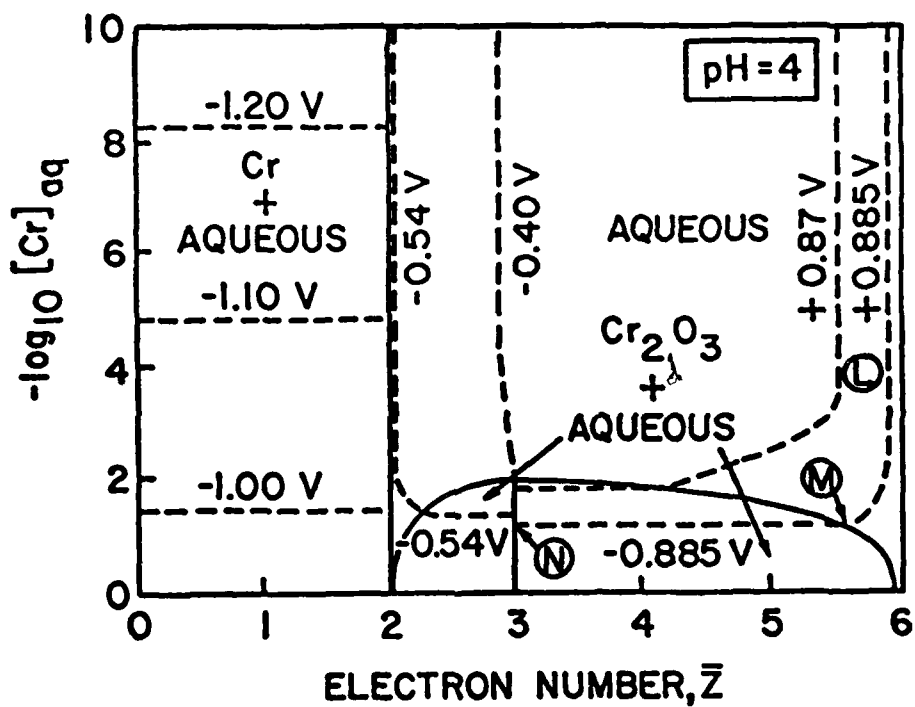


Figure 5-13 Electron number diagram for the chromium system. Intersection of the three dimensional figure with the  $\text{pH} = 4$  plane. Evaporation trajectory of a solution held at  $0.885\text{ V}$  ( $\approx 0.05\text{ ppm O}_2$  in  $\text{N}_2$ ) is shown along the line  $\overline{\text{LMN}}$ .

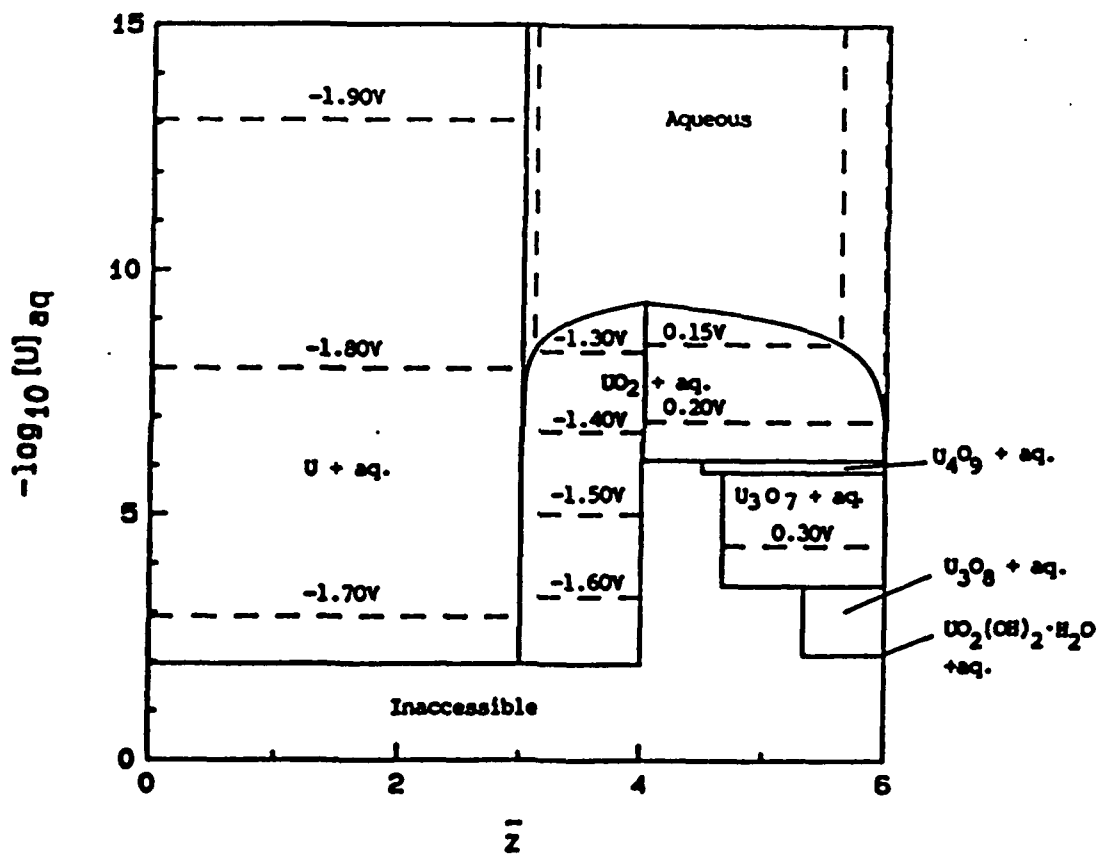


Figure 5-14 Electron number diagram for the aqueous uranium system at  $\text{pH} = 4$ .

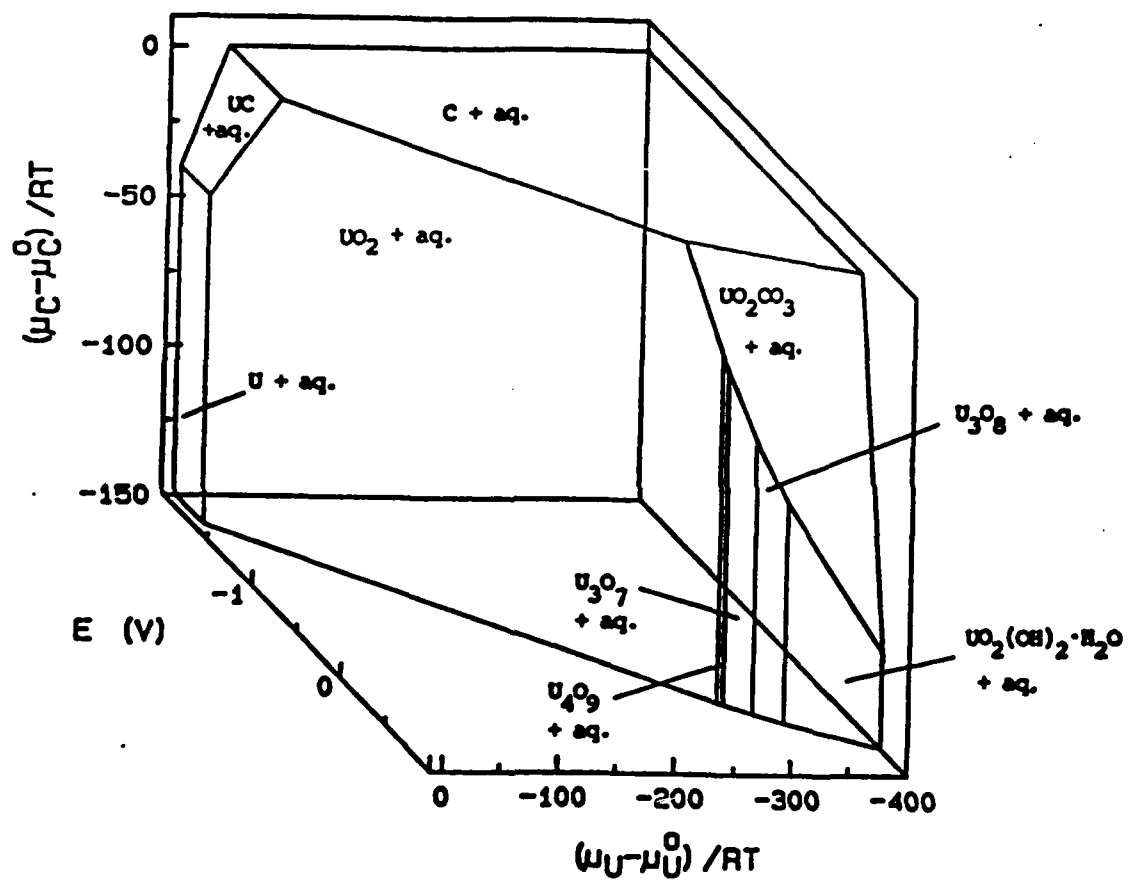


Figure 5-15 Equilibrium diagram for the aqueous U-C system at pH =4 in chemical potential space.

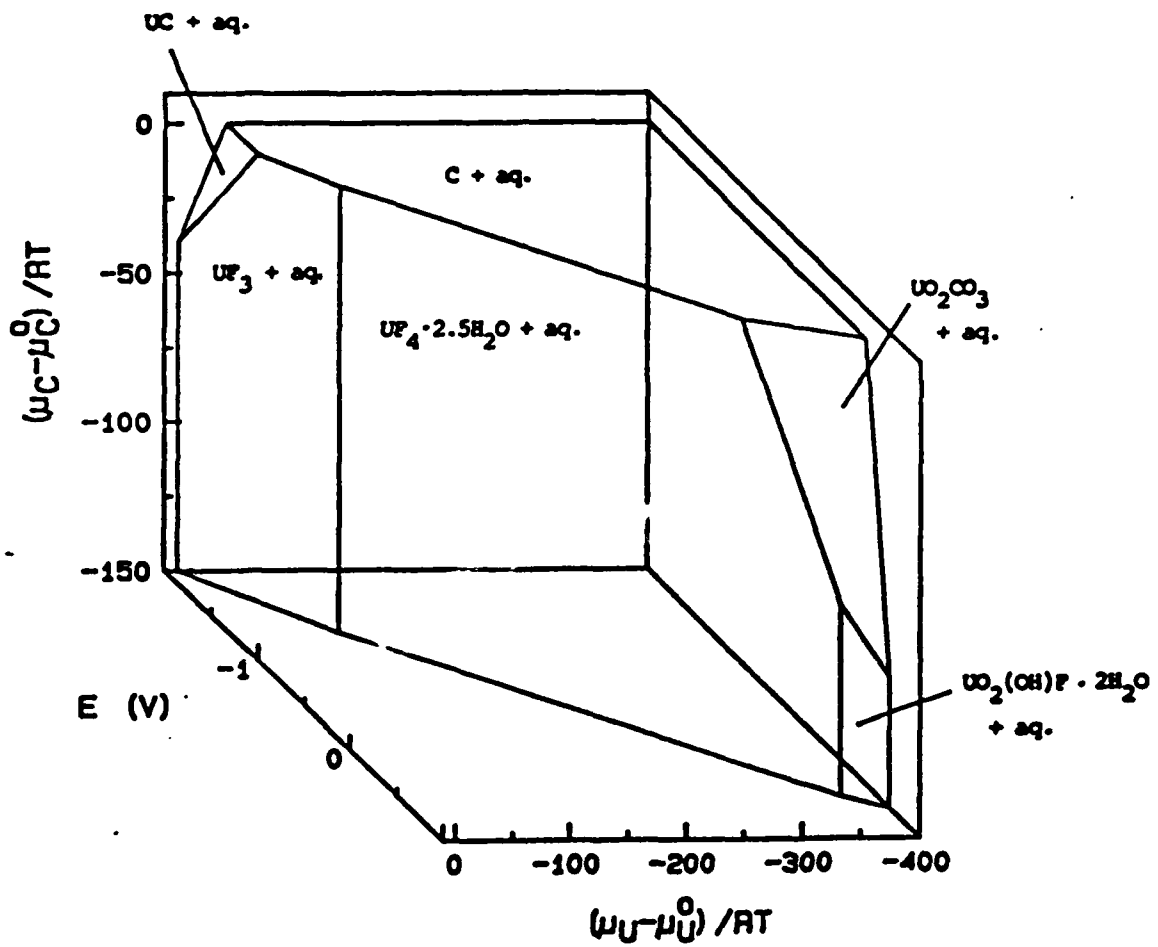


Figure 5-16 Equilibrium diagram for the aqueous U-C-F<sup>-</sup> system at pH = 4 and  $a_{F^-} = 0.1$  in chemical potential space.

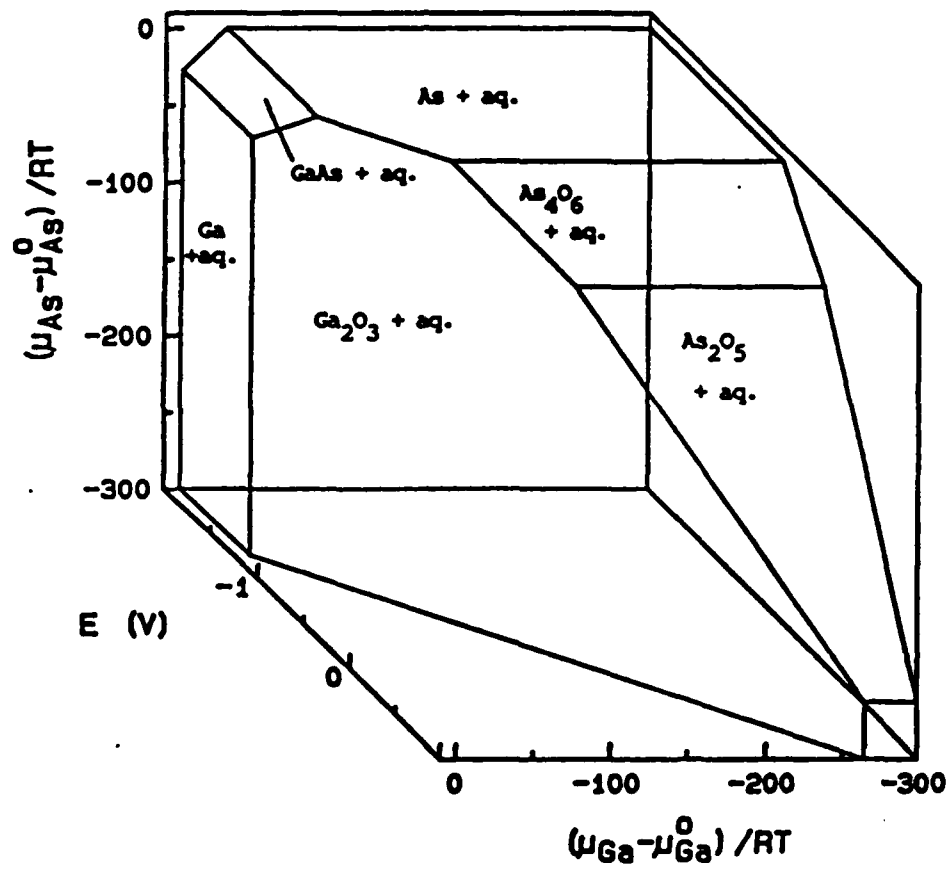


Figure 5-17 Equilibrium diagram for the aqueous Ga-As system at pH = 13 in chemical potential space.

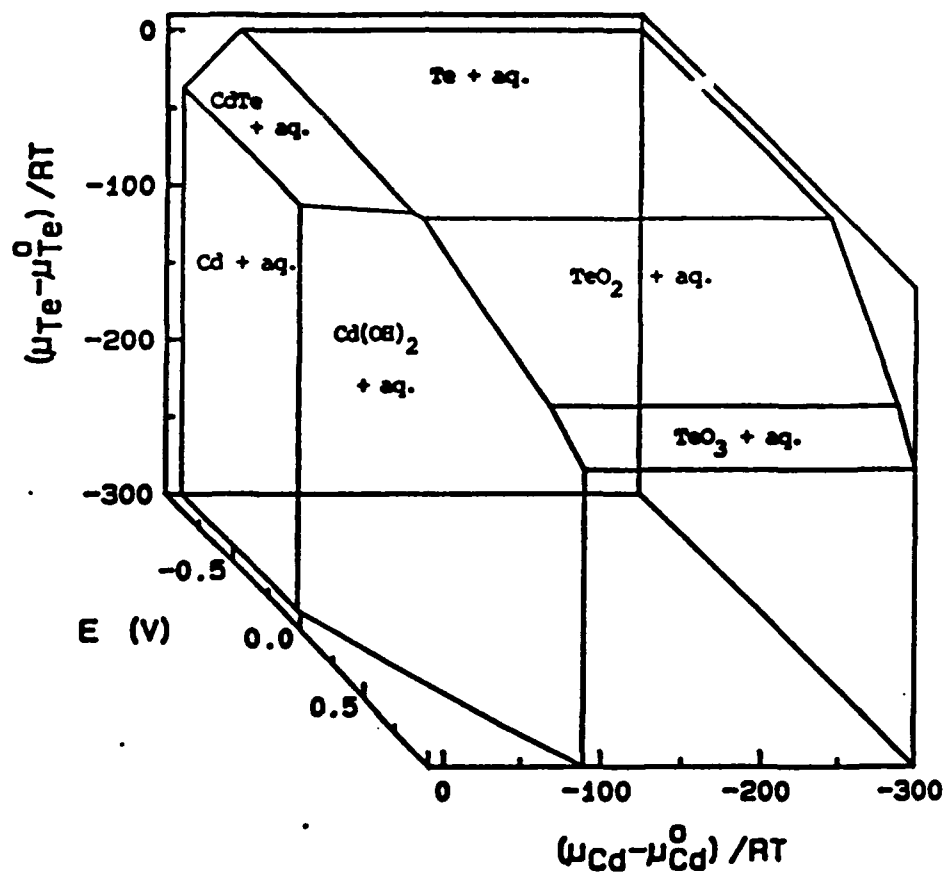


Figure 5-18 Equilibrium diagram for the aqueous Cd-Te system at pH = 2.5 in chemical potential space.

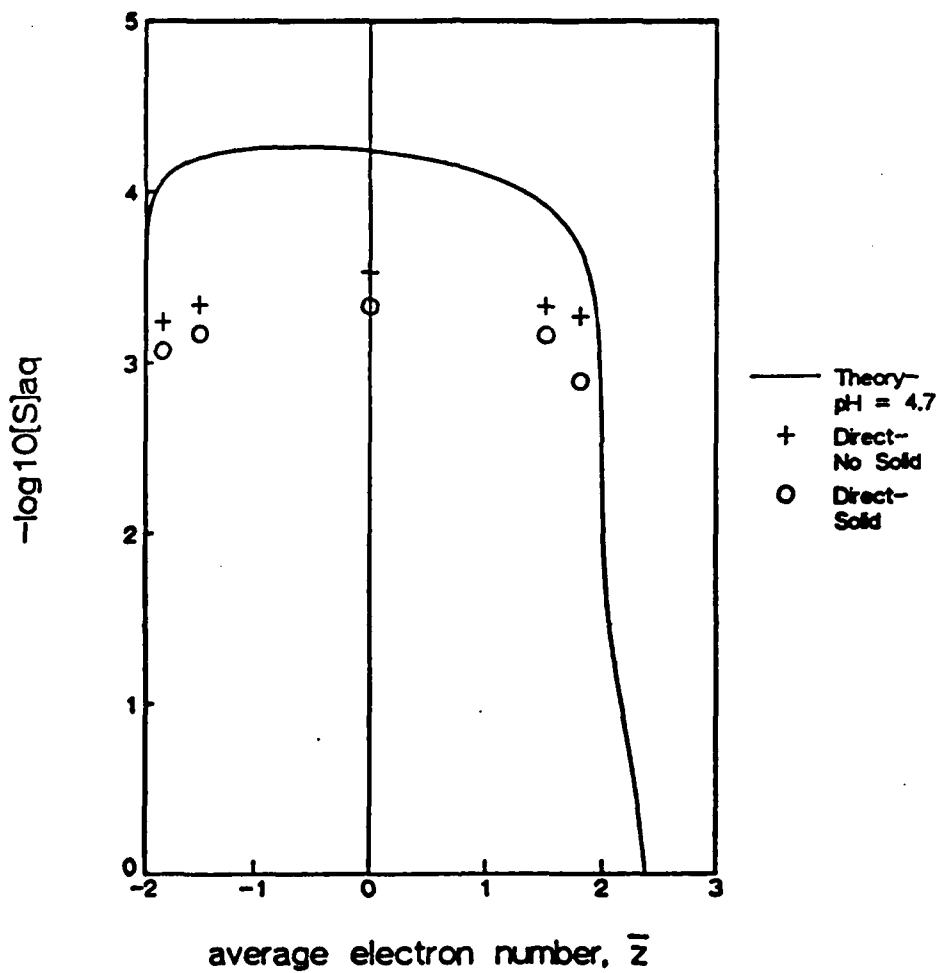


Figure 6-1 Results of direct determination experiments for the aqueous sulfur system at  $\text{pH} = 4.7 \pm 0.5$ . The solid line is the theoretical curve. Experimental data are indicated by symbols: "o"'s indicate points where solid formation was observed; at points indicated by "+"'s, no solid formation was observed.

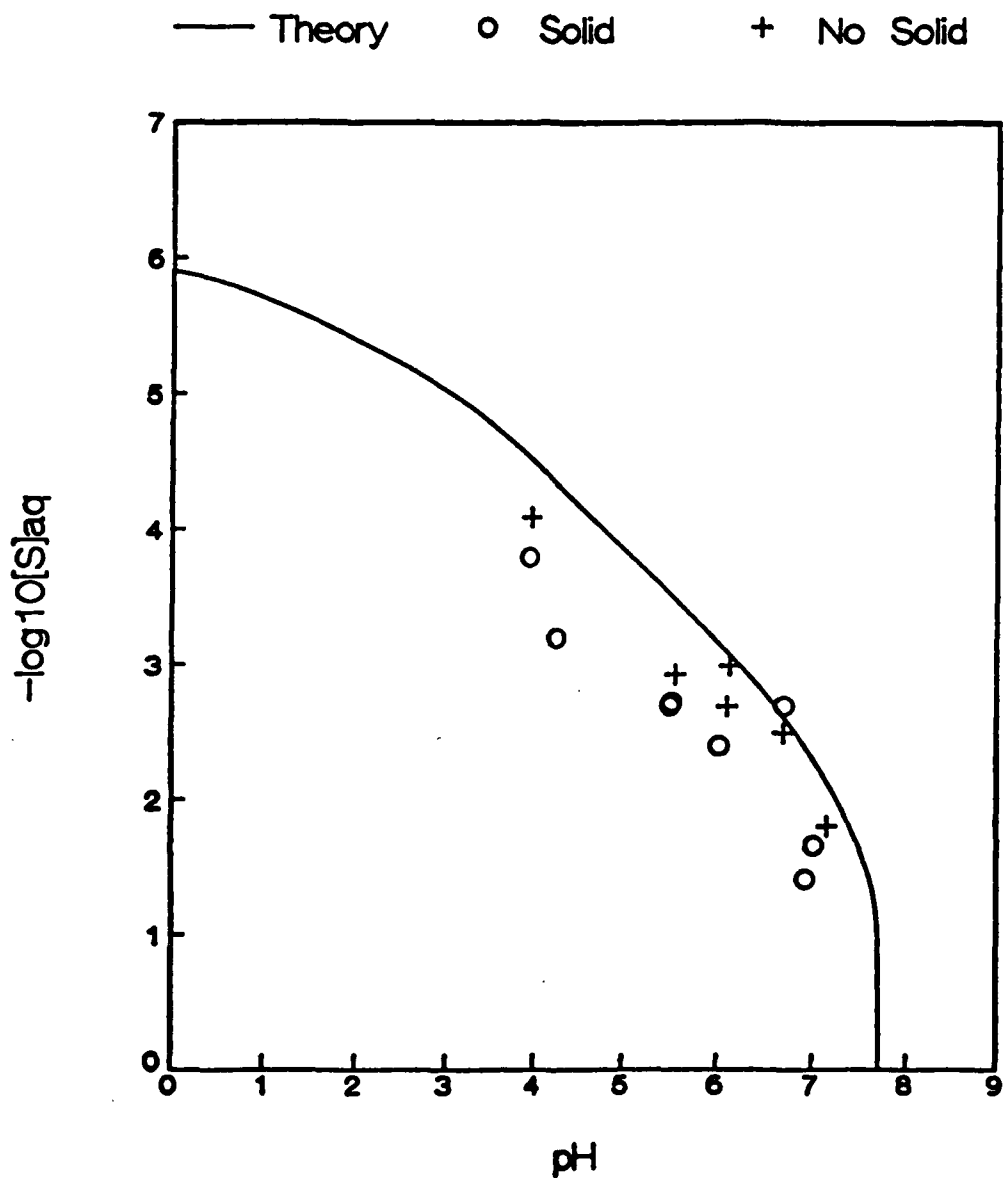


Figure 6-2 Results of direct determination experiments for the aqueous sulfur system at  $\bar{s} = -1.85$ . The solid line is the theoretical curve. Experimental data are indicated by symbols: "o"s indicate points where solid formation was observed; at points indicated by "+"s, no solid formation was observed.